

The Influence of Soil Moisture and Surface Roughness on an Idealized Tropical Cyclone

A. M. Thomas¹, J. M. Shepherd¹, and J. A. Santanello²

¹Department of Geography, University of Georgia, Athens, GA, USA

²Hydrological Sciences Laboratory, NASA's Goddard Space Flight Center, Greenbelt, MD, USA

Corresponding author: Andrew Thomas (amt59022@uga.edu)

Key Points:

- Increases in surface roughness can increase precipitation, but at the cost of maximum wind speed.
- Intensity is more sensitive to soil moisture in areas with a low surface roughness, while the precipitation is more sensitive to areas with a higher surface roughness.
- Soil moisture gradients were shown to have a larger impact on tropical cyclone precipitation in areas with a higher surface roughness.

Abstract

On occasion, tropical cyclones (TCs) have been shown to strengthen over land, provided that the land is warm and moist. The emergent hypothesis is that the moist surface provides sustaining latent heat flux that is reminiscent of an oceanic environment. To test this hypothesis, numerical simulations of idealized TCs with various profiles of soil moisture availability (SMA) and surface roughness were conducted. SMA gradients are shown to have a large influence on precipitation beyond uniform SMA. The sensitivity of accumulated precipitation to SMA is larger with enhanced friction. The maximum wind speed is more sensitive to differences in SMA under lower surface roughness. Results provide a foundation for refining emerging theories about land–atmosphere interactions with landfalling tropical systems. Additionally, these findings may inform forecasters to consider land-surface conditions when assessing intensity trends for landfalling tropical cyclones, particularly since assimilation of soil moisture and surface characteristics can yield differing impacts.

Plain Language Summary

An emerging set of studies have shown that some tropical cyclones either maintain their intensity or strengthen over land. The idea is that in areas with a large amount of soil moisture, the water evaporated from the surface can mimic an ocean environment and impact the cyclone. In order to investigate this emerging concept, a simulation of a hurricane within a controlled box was conducted with a weather model. An array of additional experiments were conducted with various land conditions and soil moisture instead of water. It was found that more precipitation, but weaker winds, were found in the hurricane over cropland rather than bare ground. Spatial differences in soil moisture were also very influential to rainfall, especially for accumulated rainfall.

1 Introduction

It is commonly accepted that a tropical cyclone (TC) typically dissipates after landfall (John Kaplan & DeMaria, 1995; Zhu, 2008) unless it undergoes extratropical transition (Evans et al., 2017; Keller et al., 2018). The reasons for the dissipation include the absence of moisture source (Shen et al., 2002; Tuleya & Kurihara, 1978), and the existence of shear (J. Kaplan & Demaria, 2001). The influence of soil moisture may slow the dissipation to a negligible rate, and even reverse the dissipation rate while maintaining characteristics of a TC (Andersen et al., 2013; Andersen & Shepherd, 2014; Arndt et al., 2009; Nair et al., 2019). This is termed the Brown Ocean Effect (BOE), as the ground surface is presumed to be so moist and warm, that the moisture flux is comparable to that from over an ocean (Andersen et al., 2013). The impact of the BOE is not a binary categorization, but rather a signal with a spectrum of influence (Yoo et al., 2020). The BOE differs from other studies that hypothesize the existence of cyclogenesis over land (Cronin & Chavas, 2019; Mrowiec et al., 2011), in that the tropical cyclone has been formed a priori and is influenced by surface fluxes post-landfall.

The BOE hypotheses have primarily assumed a constant soil moisture distribution. However, the assumption of uniform soil moisture is not appropriate for a realistic environment, but is still consistent within the literature that supports the BOE (Andersen & Shepherd, 2014). Previous studies that examined the influence of soil moisture gradients on TCs include Tropical Storm Erin (2007; Arndt et al., 2009; Kellner et al., 2012; Monteverdi & Edwards, 2010) and Hurricane Danny (1997) and Hurricane Fran (1996) (Kehoe et al., 2010). Kellner et al. (2012)

hypothesized that the soil moisture gradient helped produce a gradient in vorticity, which helped to reintensify Tropical Storm Erin, which studies have suggested to be a BOE case (Arndt et al., 2009; Monteverdi & Edwards, 2010). This finding is consistent with Evans et al. (2011). Kehoe et al. (2010) proposed that the enhancement of Hurricane Fran was due to soil moisture gradients, drawing from an analogy of other mesoscale circulations induced by differences in land use (Hong et al., 1995; Ookouchi et al., 1984). Kehoe et al. (2010) also indicated that Hurricane Danny had local maxima in precipitation in areas where the soil moisture gradient was prominent.

Previous studies also suggest that the intensity of TCs is dependent on the surface drag coefficient (Bryan, 2013; Emanuel, 1995; Malkus & Riehl, 1960). The surface drag coefficient is dependent on surface roughness length and the Monin-Obukhov length (Powell et al., 2003; Stull, 2009). The surface roughness is a featural difference between the land surface and oceanic surface which is another aspect in which the BOE is different from the typical intensification of TCs. Changes in the roughness length may reduce tropical cyclone intensity overall, but may also induce convergence, enhancing local winds (Zhu, 2008). Increases in surface drag have also been proposed to be a mechanism for the enhancement of precipitation in tropical cyclones (Zhang et al., 2018).

The goal of this research is to demonstrate the validity of the BOE from a theoretical perspective, as well as test the aforementioned deviations from a typical water surface, which is conducive to tropical cyclone intensification, to a land surface with varying characteristics. A simulation of an idealized tropical cyclone was used to conduct a series of experiments replacing the water surface with surface roughness and patterns of soil moisture availability (SMA; Lee & Pielke, 1992) beneath a developed cyclone. Section 2 provides an overview of the data and methodology, and results are presented in section 3. Section 4 summarized key conclusions and points of discussion.

2 Data and Methods

The Weather Research and Forecasting Model (WRF) version 3.8 was used to simulate an idealized TC. Specific changes to the default configuration of WRF include the deactivation of radiation, convective, and land-surface parameterization, as well as a domain of 984 km x 984 km with 4 km resolution. A control simulation (CTRL) with a water surface was run for a 10 day period. After a two day period, the restart file of CTRL was altered by replacing the water surface with different land-use types and SMA profiles. Two different land-use categories were used, namely “Bare Ground” (BG; $z_0=0.01$ m) and “Mixed Cropland” (MC; $z_0=0.1$ m) land use types. Since the land-surface parameterization was deactivated, the SMA profile was non-variant with unintended feedback mechanisms suppressed. One limitation with this approach is that while the TC may move, the soil moisture profile does not change. Eleven of the fourteen SMA profiles consisted of uniform SMA, ranging from 0 to 1. Three non-uniform SMA profiles were also used: a parabolically weighted Gaussian distribution (wG), inverse of the weighted Gaussian distribution (iwG), and piecewise (Pw). Those three non-uniform SMA profiles are described by Table 1, where x' and y' are normalized coordinates relative to the minimum central pressure, and R is the radius from the minimum central pressure. Particular simulations will be referred to as land use type, followed by the SMA profile. For example, BG-wG will refer to the bare ground simulation with the weighted Gaussian distribution and MC-U0.3 will refer to the mixed cropland simulation with a uniform SMA of 0.3.

Table 1: Details and equations describing the non-uniform soil moisture availability profiles.

Long Name	Abbreviated Name	Expression	Reason
Parabolically weighted Gaussian	wG	$\left(1 - \frac{[x']^2}{2} - \frac{[y']^2}{2}\right) \exp\left(-\frac{[x']^2}{2} - \frac{[y']^2}{2}\right)$	Moist near center, dry at edge of domain
Inverse weighted Gaussian	iwG	$1 - \left(1 - \frac{[x']^2}{2} - \frac{[y']^2}{2}\right) \exp\left(-\frac{[x']^2}{2} - \frac{[y']^2}{2}\right)$	Dry near center, moist at edge of domain
Piecewise	Pw	$\begin{cases} 0 & \text{if } R > 250 \text{ km} \\ 1 & \text{if } R < 250 \text{ km} \end{cases}$	Moist near center. Strongest SMA gradient.

3 Results

Figure 1 shows the maximum instantaneous wind speed for the BG and MC land use types for all 14 SMA profiles. CTRL achieves an asymptotically stable (Kieu, 2015) quasi-steady state (QSS) shortly after rapid intensification. Although CTRL achieves a QSS, the BOE experiments decay at varying rates, consistent with Kaplan & DeMaria (1995). As expected, the maximum wind speed for all of the BG simulations were generally greater than the MC simulations. One important difference between the CTRL simulation and the BG/MC simulations is the onset of rapid intensification (RI), which is defined as the increase of the maximum wind speed by 30 knots in 24 hours or less. RI onset occurs earlier in the BG/MC simulations, with the exception of the iwG and drier uniform SMA distributions of the BG simulations. The onset of RI happens earlier in the MC simulations than the CTRL. Moreover, the BG-wG and BG-Pw have a more pronounced period of RI. The maximum wind speed of the uniform BG simulations during the QSS are more incremental than the MC simulations, which shows less distinguishable pattern. To this extent, the maximum wind speed in the QSS for the MC-Pw and MC-iwG simulations are almost indistinguishable. The maximum wind speed in the BG simulations during the QSS are more sensitive to changes in the SMA, especially near the center of the TC, than the MC simulations.

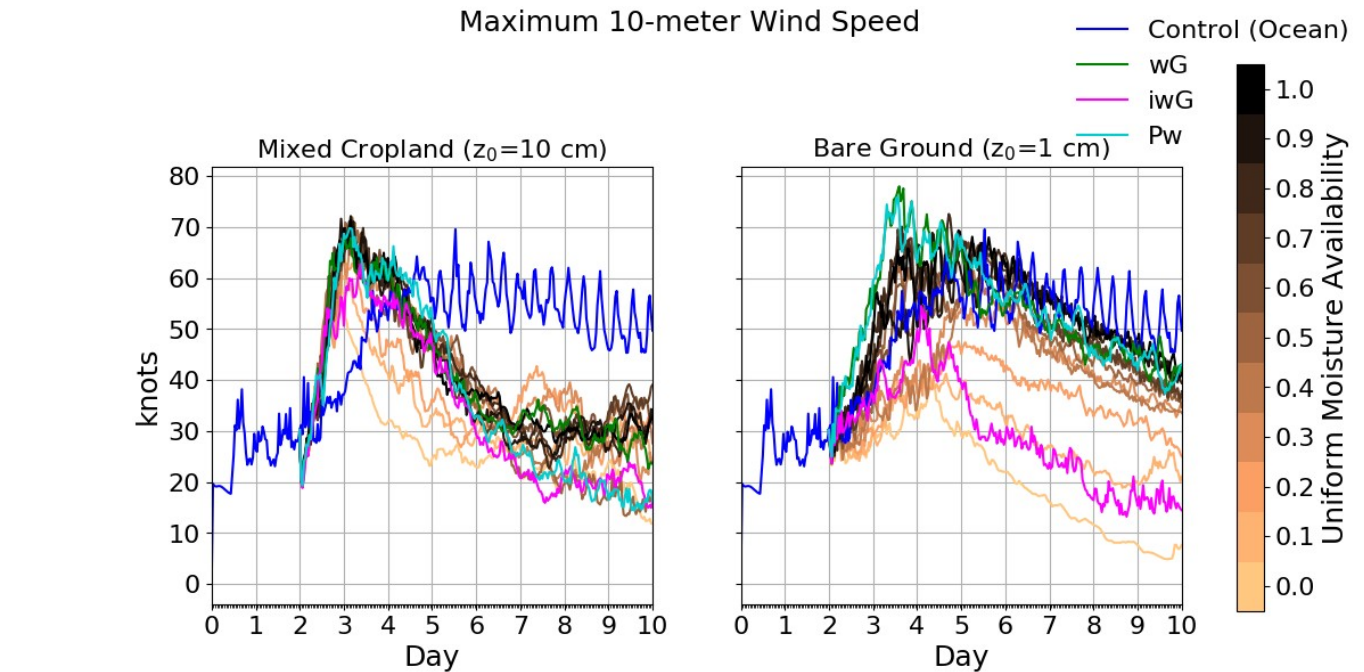


Figure 1: Maximum instantaneous wind speed (knots) for idealized tropical cyclones over a water surface (CTRL), over Mixed Cropland (left) and Bare Ground (right). The uniform SMA profiles are labeled according to the colorbar, while the CTRL and non-uniform SMA profiles are labeled in the legend.

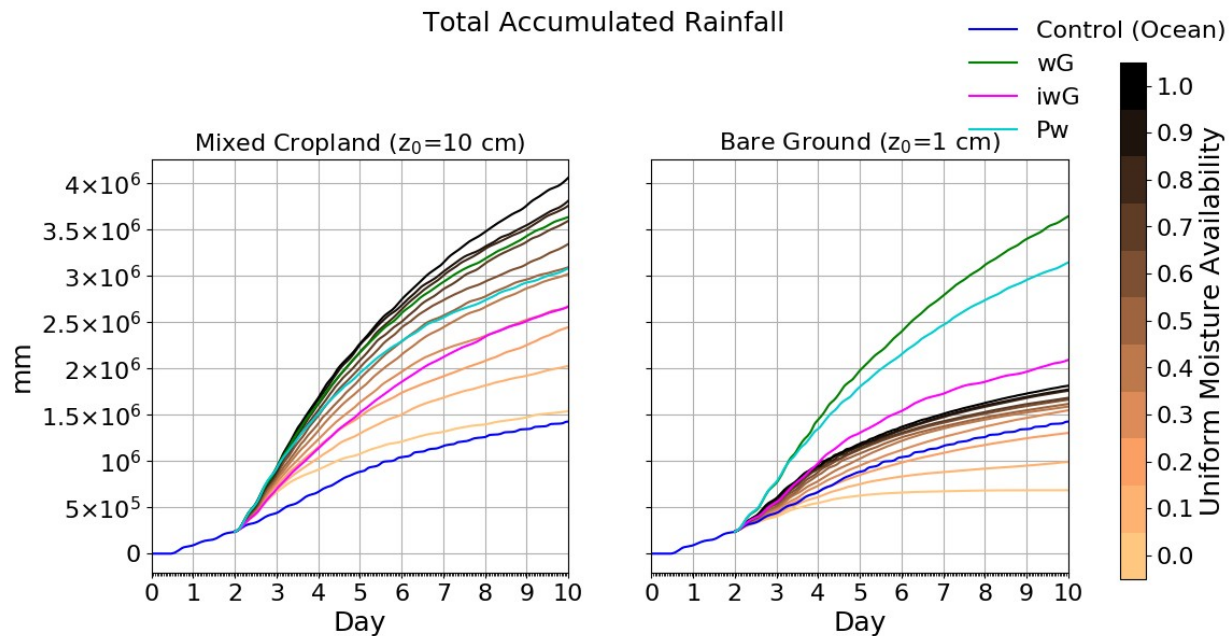


Figure 2: Domain-summed accumulated precipitation (mm) for idealized tropical cyclones over a water surface (CTRL), over Mixed Cropland (left) and Bare Ground (right). The uniform SMA profiles are labeled according to the colorbar, while the CTRL and non-uniform SMA profiles are labeled in the legend.

Figure 2 shows the domain-summed total accumulated precipitation over MC (left) and BG (right). All of the MC simulations produced more precipitation than the CTRL simulation. The CTRL simulation, however, produced more precipitation simulations with a lower SMA than the BG-U0.3. The presence of a gradient in SMA had a large impact in the total accumulated precipitation. The influence of the land use type was stronger on the uniform SMA profiles than the SMA profiles that had a SMA gradient. That is, the BG-iwG produced more precipitation than the BG-U1.0, while the MC-U1.0 produced more precipitation than the MC-wG. Land use has a small impact on the total accumulated precipitation generated by SMA gradients. BG-wG and MC-wG, as well as MC-Pw and BG-Pw, have comparable total accumulated rainfall amounts, however MC-iwG produced more precipitation than BG-iwG indicating that there may be a radial dependence to this relationship. The cause of this is likely due to the differences in sensitivity of the surface latent heat flux.

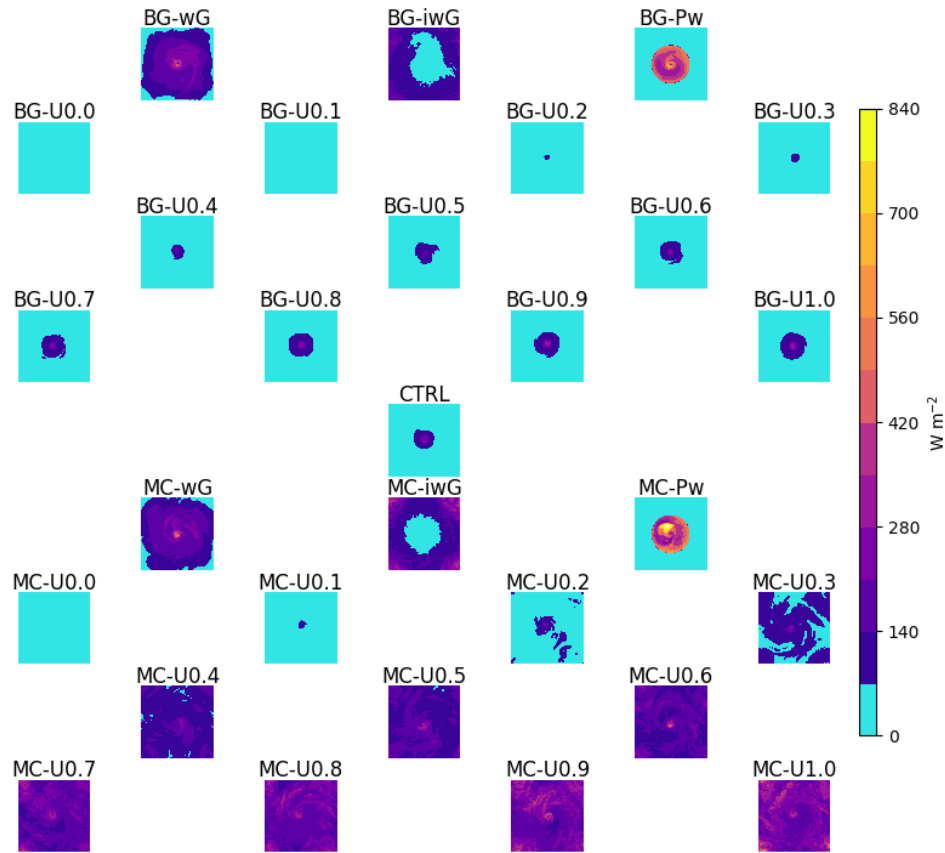


Figure 3: Surface latent heat flux (W m^{-2}) for each simulation at hour 180.

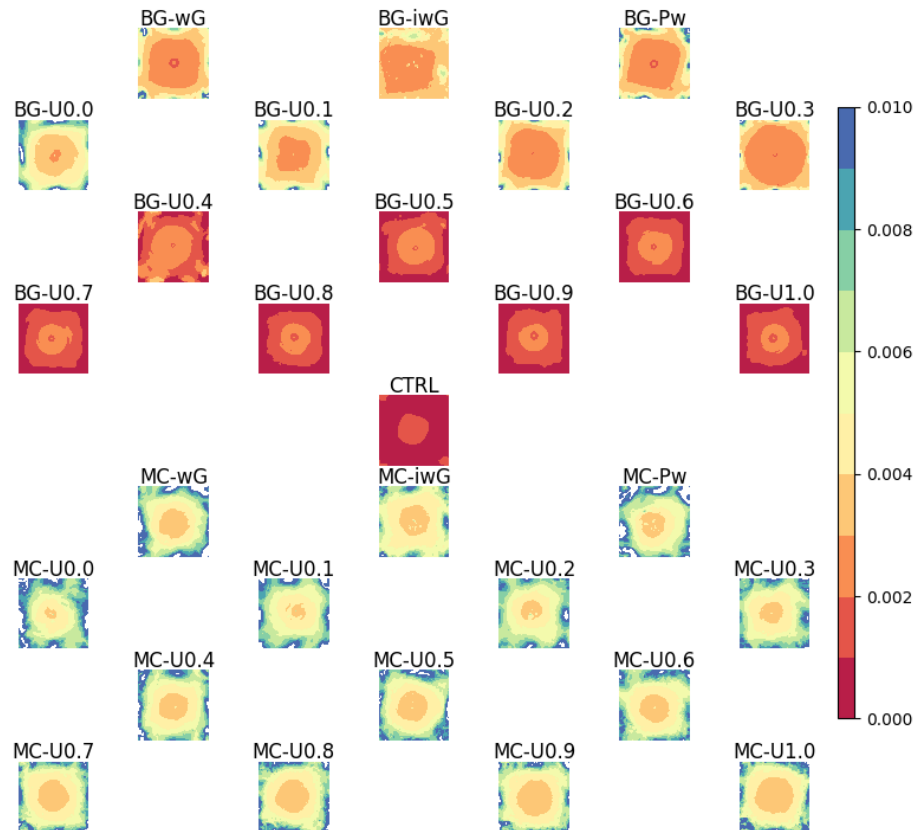


Figure 4: Enthalpy exchange coefficient after 180 hours of the CTRL simulation.

Figure 3 shows the surface latent heat flux, which is computed by the surface layer parameterization, after 180 hours of the CTRL simulation. This demonstrates that the latent heat flux of the MC-U0.2 and BG-U0.5 most resemble the latent heat flux of the CTRL simulation. Latent heat flux increase is larger in the MC simulations than the BG simulations, even though the wind speed is lower. The cause of the difference in latent heat flux between land-use categories is due to enhancements in the bulk enthalpy transfer coefficient, depicted by Figure 4. The greatest amount of latent heat flux is found in the simulations with the Pw profile. The Pw SMA profiles also have the largest gradient in latent heat flux, as expected with the gradient in the SMA profile. The enhanced soil moisture gradient allows dry air from outside the radius to be advected within the storm, enhancing the moisture gradient between the surface and lower atmosphere, further increasing the latent heat flux.

4 Discussion and Conclusions

Through the use of idealized simulations of tropical cyclones, the plausibility of the BOE was confirmed. The explanatory power of the BOE through the enhancements of latent heat flux ignores the reality of SMA gradients, which can produce more precipitation than the BOE itself in areas with a lower roughness length. Moreover, increases in friction enhance the precipitation produced, at the cost of hurricane intensity. Thus, it is proposed that the BOE should be evaluated among two different modes, precipitation enhancement and intensification/maintenance. The pattern of the sudden enhancement of RI due to heightened surface friction is consistent with Montgomery et al. (2010), and the reduction in the QSS is

consistent with Bryan (2013). Enhancements in precipitation are more likely in areas that have more friction and weaker wind speeds. The effect of friction on precipitation suggests that hurricane-related flooding is enhanced in urbanized areas, which is consistent with the study by Zhang et al. (2018) on Hurricane Harvey.

Some caveats should be mentioned concerning this study. This was a modeling study in an idealized environment, so the conditions may not perfectly align in observational studies. This includes the expanse of one singular land use type, as well as the validity of parameterizations used by the simulation, and the presence of environmental shear. Some of the assumptions used also may reduce feedback mechanisms (such as evaporative cooling decreasing in surface temperature) that could be an artefact of a stagnant tropical cyclone rather than a tropical cyclone moving over an infinite expanse. Deactivating these settings also eliminates potentially relevant feedback mechanisms and signals (Subramanian, 2016; Tang et al., 2019; Tang & Zhang, 2016). This experiment also does not test changes to surface temperature or gradients in surface temperature. Also, the method of replacing the land surface does not induce asymmetries typical of a landfalling tropical cyclone. Despite these shortcomings, these simulations demonstrate the importance of having accurate representation of soil moisture profile and surface features.

Acknowledgments, Samples, and Data

This research was supported by the NASA Modeling, Analysis, and Prediction (MAP) program (16-MAP16-013). Computations were completed through the Georgia Advanced Computing Research Center. We are thankful for the anonymous reviewers for their input.

References

- Andersen, T. K., & Shepherd, J. M. (2014). A global spatiotemporal analysis of inland tropical cyclone maintenance or intensification. *International Journal of Climatology*. <https://doi.org/10.1002/joc.3693>
- Andersen, T. K., Radcliffe, D. E., & Shepherd, J. M. (2013). Quantifying surface energy fluxes in the vicinity of inland-tracking tropical cyclones. *Journal of Applied Meteorology and Climatology*, 52(12), 2797–2808. <https://doi.org/10.1175/JAMC-D-13-035.1>
- Arndt, D. S., Basara, J. B., McPherson, R. A., Illston, B. G., McManus, G. D., & Demko, D. B. (2009). Observations of the Overland Reintensification of Tropical Storm Erin (2007). *Bulletin of the American Meteorological Society*, 90(8), 1079–1094. <https://doi.org/10.1175/2009BAMS2644.1>
- Bryan, G. H. (2013). Notes and correspondence comments on “sensitivity of tropical-cyclone models to the surface drag coefficient.” *Quarterly Journal of the Royal Meteorological Society*, 139(676), 1957–1960. <https://doi.org/10.1002/qj.2066>
- Cronin, T. W., & Chavas, D. R. (2019). Dry and Semidry Tropical Cyclones. *Journal of the Atmospheric Sciences*, 76(8), 2193–2212. <https://doi.org/10.1175/jas-d-18-0357.1>
- Emanuel, K. A. (1995). Sensitivity of Tropical Cyclones to Surface Exchange Coefficients and a Revised Steady-State Model incorporating Eye Dynamics. *Journal of the Atmospheric Sciences*, 52(22), 3969–3976. <https://doi.org/10.1175/1520->

- 206 0469(1995)052<3969:SOTCTS>2.0.CO;2
- 207 Evans, C., Schumacher, R. S., & Galarneau, T. J. (2011). Sensitivity in the Overland
208 Reintensification of Tropical Cyclone Erin (2007) to Near-Surface Soil Moisture
209 Characteristics. *Monthly Weather Review*. <https://doi.org/10.1175/2011MWR3593.1>
- 210 Evans, C., Wood, K. M., Aberson, S. D., Archambault, H. M., Milrad, S. M., Bosart, L. F., et al.
211 (2017). The extratropical transition of tropical cyclones. Part I: Cyclone evolution and direct
212 impacts. *Monthly Weather Review*, 145(11), 4317–4344. [https://doi.org/10.1175/MWR-D-](https://doi.org/10.1175/MWR-D-17-0027.1)
213 17-0027.1
- 214 Hong, X., Leach, M. J., & Raman, S. (1995). Role of vegetation in generation of mesoscale
215 circulation. *Atmospheric Environment*, 29(16), 2163–2176. [https://doi.org/10.1016/1352-](https://doi.org/10.1016/1352-2310(94)00241-C)
216 2310(94)00241-C
- 217 Kaplan, J., & Demaria, M. (2001). On the decay of tropical cyclone winds after landfall in the
218 New England Area. *Journal of Applied Meteorology*, 40(2), 280–286.
219 [https://doi.org/10.1175/1520-0450\(2001\)040<0280:OTDOTC>2.0.CO;2](https://doi.org/10.1175/1520-0450(2001)040<0280:OTDOTC>2.0.CO;2)
- 220 Kaplan, John, & DeMaria, M. (1995). A Simple Empirical Model for Predicting the Decay of
221 Tropical Cyclone Winds after Landfall. *Journal of Applied Meteorology*, 34(11), 2499–
222 2512. [https://doi.org/10.1175/1520-0450\(1995\)034<2499:ASEMFP>2.0.CO;2](https://doi.org/10.1175/1520-0450(1995)034<2499:ASEMFP>2.0.CO;2)
- 223 Kehoe, J., Raman, S., & Boyles, R. (2010). Characteristics of landfalling tropical cyclones in
224 North Carolina. *Marine Geodesy*, 33(4), 394–411.
225 <https://doi.org/10.1080/01490419.2010.518059>
- 226 Keller, J. H., Grams, C. M., Riemer, M., Archambault, H. M., Bosart, L., Doyle, J. D., et al.
227 (2018). The Extratropical Transition of Tropical Cyclones. Part II: Interaction with the
228 Midlatitude Flow, Downstream Impacts, and Implications for Predictability. *Monthly*
229 *Weather Review*, 147(4), 1077–1106. <https://doi.org/10.1175/mwr-d-17-0329.1>
- 230 Kellner, O., Niyogi, D., Lei, M., & Kumar, A. (2012). The role of anomalous soil moisture on
231 the inland reintensification of Tropical Storm Erin (2007). *Natural Hazards*, 63(3), 1573–
232 1600. <https://doi.org/10.1007/s11069-011-9966-6>
- 233 Kieu, C. (2015). Hurricane maximum potential intensity equilibrium. *Quarterly Journal of the*
234 *Royal Meteorological Society*, 141(692), 2471–2480. <https://doi.org/10.1002/qj.2556>
- 235 Lee, T. J., & Pielke, R. A. (1992). Estimating the soil surface specific humidity. *Journal of*
236 *Applied Meteorology*. [https://doi.org/10.1175/1520-](https://doi.org/10.1175/1520-0450(1992)031<0480:ETSSSH>2.0.CO;2)
237 0450(1992)031<0480:ETSSSH>2.0.CO;2
- 238 Malkus, J. S., & Riehl, H. (1960). On the Dynamics and Energy Transformations in Steady-State
239 Hurricanes. *Tellus*, 12(1), 1–20. <https://doi.org/10.3402/tellusa.v12i1.9351>
- 240 Monteverdi, J. P., & Edwards, R. (2010). The Redevelopment of a Warm-Core Structure in Erin:
241 A Case of Inland Tropical Storm Formation. *E-Journal of Severe Storms Meteorology*, 5(6),

- 242 1–18. Retrieved from <http://ejssm.org/ojs/index.php/ejssm/article/viewArticle/65>
- 243 Montgomery, M. T., Smith, R. K., & Nguyen, S. V. (2010). Sensitivity of tropical-cyclone
244 models to the surface drag coefficient. *Quarterly Journal of the Royal Meteorological*
245 *Society*, 136(653), 1945–1953. <https://doi.org/10.1002/qj.702>
- 246 Mrowiec, A. A., Garner, S. T., & Pauluis, O. M. (2011). Axisymmetric Hurricane in a Dry
247 Atmosphere: Theoretical Framework and Numerical Experiments. *Journal of the*
248 *Atmospheric Sciences*. <https://doi.org/10.1175/2011JAS3639.1>
- 249 Nair, U. S., Rappin, E., Foshee, E., Smith, W., Pielke, R. A., Mahmood, R., et al. (2019).
250 Influence of Land Cover and Soil Moisture based Brown Ocean Effect on an Extreme
251 Rainfall Event from a Louisiana Gulf Coast Tropical System. *Scientific Reports*, 9(1),
252 17136. <https://doi.org/10.1038/s41598-019-53031-6>
- 253 Ookouchi, Y., Segal, M., Kessler, R. C., & Pielke, R. A. (1984). Evaluation of soil moisture
254 effects on the generation and modification of mesoscale circulations. *Monthly Weather*
255 *Review*. [https://doi.org/10.1175/1520-0493\(1984\)112<2281:EOSMEO>2.0.CO;2](https://doi.org/10.1175/1520-0493(1984)112<2281:EOSMEO>2.0.CO;2)
- 256 Powell, M. D., Vickery, P. J., & Reinhold, T. A. (2003). Reduced drag coefficient for high wind
257 speeds in tropical cyclones. *Nature*, 422(6929), 279–283.
258 <https://doi.org/10.1038/nature01481>
- 259 Shen, W., Ginis, I., & Tuleya, R. (2002). A numerical investigation of land surface water on
260 landfalling hurricanes. *Journal of the Atmospheric ...*, 59(1994), 789–802.
261 [https://doi.org/10.1175/1520-0469\(2002\)059<0789:ANIOLS>2.0.CO;2](https://doi.org/10.1175/1520-0469(2002)059<0789:ANIOLS>2.0.CO;2)
- 262 Stull, R. B. (2009). *An introduction to boundary layer meteorology* (Vol. 13). Springer Science
263 & Business Media.
- 264 Subramanian, S. (2016). Modeling the impact of land surface feedbacks on post landfall tropical
265 cyclones.
- 266 Tang, X., & Zhang, F. (2016). Impacts of the diurnal radiation cycle on the formation, intensity,
267 and structure of Hurricane Edouard (2014). *Journal of the Atmospheric Sciences*, 73(7),
268 2871–2892. <https://doi.org/10.1175/JAS-D-15-0283.1>
- 269 Tang, X., Tan, Z. M., Fang, J., Munsell, E. B., & Zhang, F. (2019). Impact of the diurnal
270 radiation contrast on the contraction of radius of maximum wind during intensification of
271 Hurricane Edouard (2014). *Journal of the Atmospheric Sciences*, 76(2), 421–432.
272 <https://doi.org/10.1175/JAS-D-18-0131.1>
- 273 Tuleya, R. E., & Kurihara, Y. (1978). A Numerical Simulation of the Landfall of Tropical
274 Cyclones. *Journal of the Atmospheric Sciences*. [https://doi.org/10.1175/1520-](https://doi.org/10.1175/1520-0469(1978)035<0242:ANSOTL>2.0.CO;2)
275 [0469\(1978\)035<0242:ANSOTL>2.0.CO;2](https://doi.org/10.1175/1520-0469(1978)035<0242:ANSOTL>2.0.CO;2)
- 276 Yoo, J., Santanello, J. A., Shepherd, M., Kumar, S., Lawston, P., & Thomas, A. M. (2020).
277 Quantification of the Land Surface and Brown Ocean Influence on Tropical Cyclone

Intensification Over Land. *Journal of Hydrometeorology*, JHM-D-19-0214.1.
<https://doi.org/10.1175/JHM-D-19-0214.1>

Zhang, W., Villarini, G., Vecchi, G. A., & Smith, J. A. (2018). Urbanization exacerbated the rainfall and flooding caused by hurricane Harvey in Houston. *Nature*, 563(7731), 384–388.
<https://doi.org/10.1038/s41586-018-0676-z>

Zhu, P. (2008). Impact of land–surface roughness on surface winds during hurricane landfall. *Quarterly Journal of the Royal Meteorological Society*, 134(633), 1051–1057.
<https://doi.org/10.1002/qj.265>

[Figure 1: Maximum instantaneous wind speed for idealized tropical cyclones over a water surface \(CTRL\), over Mixed Cropland \(left\) and Bare Ground \(right\).](#)

[Figure 2: Domain-summed accumulated precipitation for idealized tropical cyclones over a water surface \(CTRL\), over Mixed Cropland \(left\) and Bare Ground \(right\).](#)

[Figure 3: Surface latent heat flux at the surface for each simulation at hour 180.](#)

[Figure 4: Enthalpy exchange coefficient after 180 hours of CTRL simulation.](#)

Table 1: Details and equations describing the non-uniform soil moisture availability profiles.